ORIGINAL ARTICLE

Value of MRI in assessing back pain after thoracolumbar osteoporotic vertebral compression fractures and discussion on the underlying mechanisms by tissue biopsy

Haoran Qi[1,5,6] · Jun Qi[2] · Ye Sun[3] · Junying Gao[4] · Jianmin Sun[1,5,6] · Guodong Wang[1]

Abstract

Purpose The specific radiological feature of osteoporotic vertebral compression fractures (OVCFs) is bone marrow oedema (BME) on magnetic resonance imaging (MRI). However, the relationship between BME and back pain (BP) is unclear. We investigated the value of MRI in assessing BP and discussed the relevant mechanisms by tissue biopsy.

Methods One hundred nineteen patients with thoracolumbar OVCFs were included in this study. We divided all patients into two groups: the low-oedema group (BME $\leq 75\%$) and the high-oedema group (BME $> 75\%$). To reduce the error generated in the acute phase of fracture, we separately analysed patients in phases I (within one month) and II (more than one month). We compared the differences between the groups using the Mann–Whitney U test and investigated the correlations using Spearman's correlation test.

Results The degree of BP was significantly correlated with BME ($p < 0.001$; $p < 0.001$) and fibrous tissue content ($p = 0.006$; $p = 0.035$) in both phases. Further, the fibrous tissue content in the low-oedema group ($12.49 \pm 7.37\%$; $15.25 \pm 13.28\%$) was significantly lower than that in the high-oedema group ($25.68 \pm 20.39\%$, $p = 0.014$; $23.92 \pm 14.61\%$, $p = 0.022$) in both phases. The lamellar bone content was significantly correlated with BP ($p = 0.021$) in phase II.

Conclusions BME signals on MRI can accurately predict the degree of BP, and the main mechanisms are related to the stimulation of fibrous tissue.

Keywords MRI · Bone marrow oedema · Back pain · Tissue microarchitecture · Osteoporotic vertebral compression fractures

✉ Jianmin Sun
   JianminSun2020@163.com

✉ Guodong Wang
   spine2019@163.com

1   Department of Spine, Shandong Provincial Hospital Affiliated to Shandong First Medical University, Jinan 250000, China

2   Laboratory Department, Jinan Infectious Diseases Hospital, Jinan 250000, China

3   Pathological Department, Jinan Infectious Diseases Hospital, Jinan 250000, China
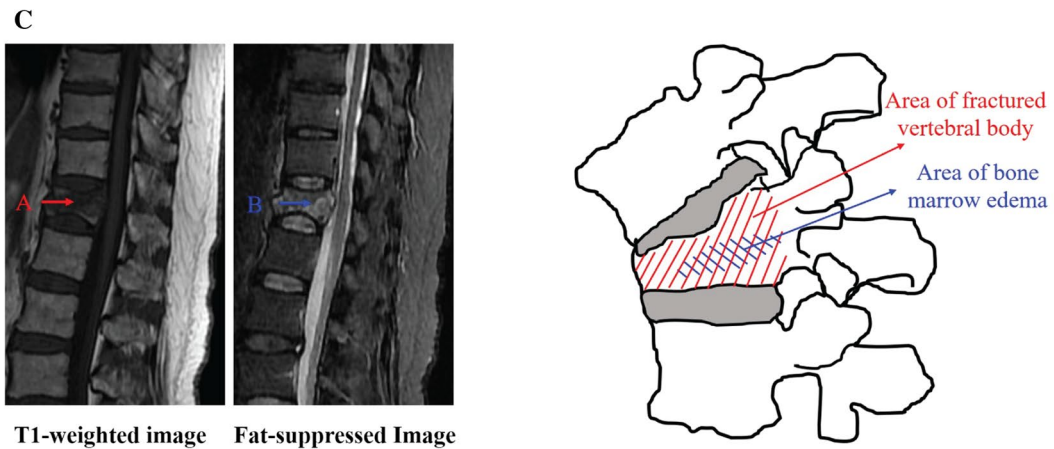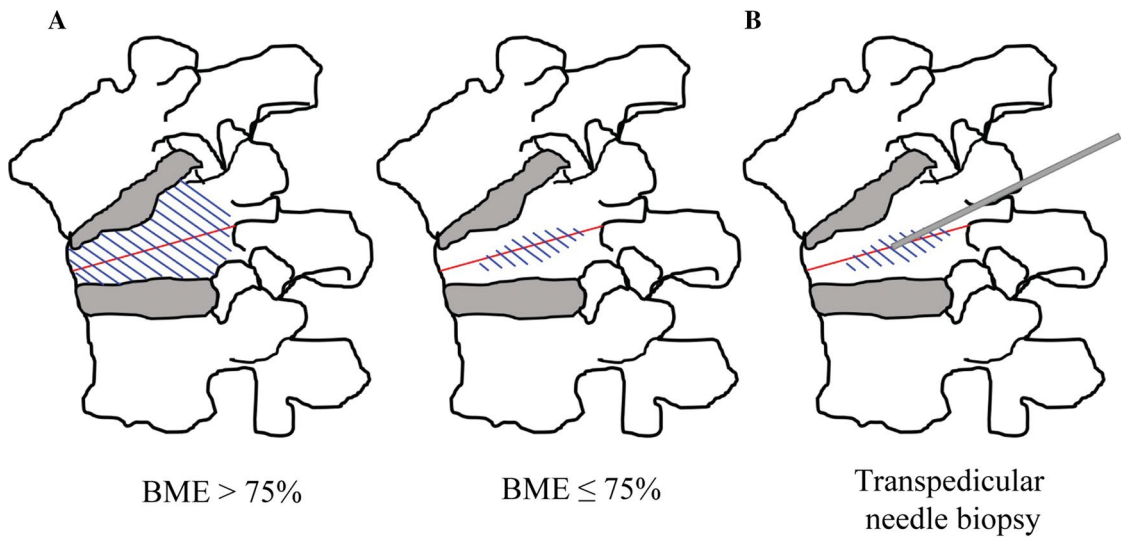
4   Ocean University of China, Qingdao 266003, China

5   Department of Spine, Shandong Provincial Hospital Affiliated to Shandong University, Jinan 250000, China
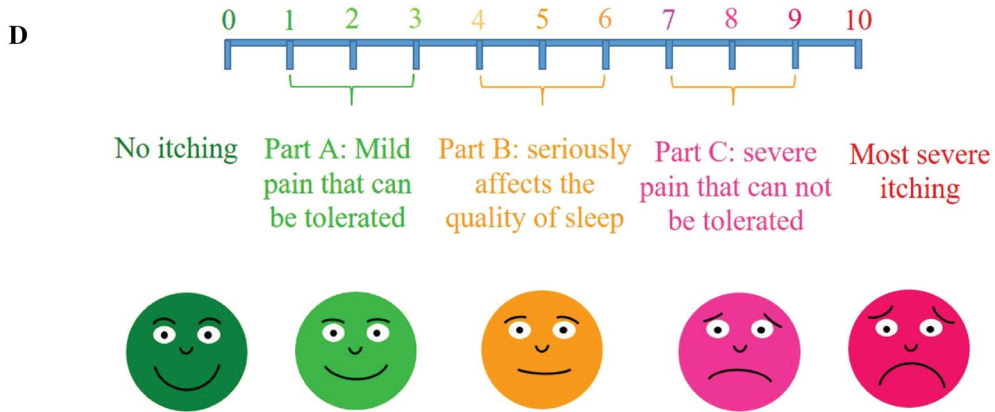
6   School of Medicine, Shandong University, Jinan 250000, China

Introduction

Osteoporotic vertebral compression fractures (OVCFs) are a common reason for limitations in mobility in the elderly population [1]. A serious complication caused by OVCFs is back pain (BP), which commonly leads to a decrease in the quality of life [2]. The degeneration of bone microarchitecture and progressive bone mineral loss are responsible for OVCFs after original trauma [3]. The incidence of OVCFs has shown an increase in the elderly Chinese population. For patients with OVCFs, accurately diagnosing the fractured vertebra before receiving surgical protocols is critical [4]. Typical imaging features of OVCFs are vertebral collapse and bone marrow oedema (BME) [5, 6]. Compared with simple X-rays and computed tomography, magnetic resonance imaging (MRI) is the most sensitive radiological examination to detect BME due to fresh fractures.

A

BME > 75%　　　　BME ≤ 75%

B

Transpedicular needle biopsy

C

T1-weighted image　Fat-suppressed Image

A: decreased signal intensity on T1-weighted images

B: increased signal intensity on fat-suppressed images

Area of fractured vertebral body

Area of bone marrow edema

$$BME \% = \frac{\text{Area of bone marrow edema}}{\text{Area of fractured vertebral body}} \times 100 \%$$

D

0　1　2　3　4　5　6　7　8　9　10

No itching　Part A: Mild pain that can be tolerated　Part B: seriously affects the quality of sleep　Part C: severe pain that can not be tolerated　Most severe itching

Visual Analoge Scale (VAS)

◄**Fig. 1** Experimental design and methods. **a** Experimental grouping according to the percentage of BME. **b** Methods of extracting tissue specimens at the fractured area. **c** Methods of measuring the percentage of BME. **d** Assessment of the severity of back pain. **a** BME: bone marrow oedema; **d** VAS: Visual Analogue Scale

Although MRI is the most sensitive radiological examination and gold standard for diagnosing OVCFs, the value of MRI for assessing BP has not been reported in the literature. This study investigated the correlations between BME and the degree of BP. We also discussed the relevant mechanisms by observing bone microarchitecture in the fractured area.
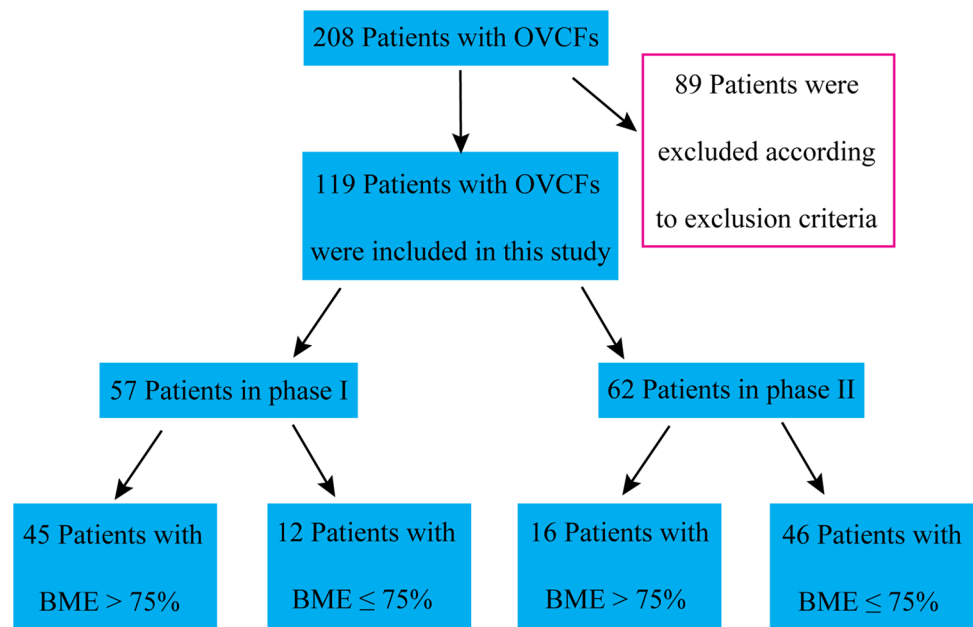
Methods

Subjects

We reviewed the medical records of all patients diagnosed with OVCFs who underwent percutaneous kyphoplasty

Fig. 2 Experimental grouping and staging. OVCFs: osteoporotic vertebral compression fractures

surgery (PKP) at our institution. According to the World Health Organization (WHO) definition criteria for OVCFs [7], we included patients with thoracolumbar OVCFs (the fractured levels were at T10 – L2) who underwent PKP surgery and from whom biopsy specimens were successfully obtained from the fractured vertebral bodies. All the patients enrolled in this study met the radiological characteristics of OVCFs [8]. The exclusion criteria were as follows: (1) pathological fractures; (2) severe traumatic fractures; (3) metabolic bone diseases; (4) recipient of anti-osteoporosis drug therapy before the surgical protocols; (5) failed to obtain biopsy specimens at the fractured area; (6) received analgesic therapy within one day before the pain assessment; and (7) multiple vertebral fractures.
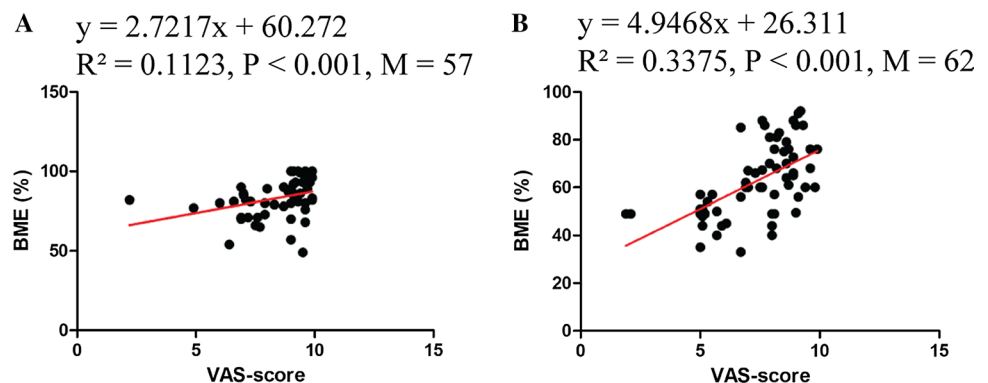
Study design

According to a previous study by Wei et al. [2], we divided all the patients into two groups based on the percentage of BME in fractured vertebral bodies (Fig. 1a): the

Fig. 3 Correlations between the percentage of BME and VAS score in phases I and II. **a** Correlations between the percentage of BME and VAS score in phase I; **b** Correlations between the percentage of BME and VAS score in phase II. *BME* bone marrow oedema

A $y = 2.7217x + 60.272$
$R^2 = 0.1123$, P < 0.001, M = 57

B $y = 4.9468x + 26.311$
$R^2 = 0.3375$, P < 0.001, M = 62

low-oedema group (BME ≤ 75%) and the high-oedema group (BME > 75%). To reduce the error generated in the acute phase of fracture, we separately analysed all the patients in phases I (less than one month from the original fracture) and II (more than one month from the original fracture). The differences in the VAS score (Visual Analogue Scale), microarchitecture content and the BME percentage between the groups were compared in the same period.

Bone tissue extraction and preservation

Because tissue biopsy techniques are often used in the clinic to identify pathological fractures, extracting bone tissue is a normal intraoperative procedure [9]. To differentiate bone tissue from pathological fractures, we routinely extracted bone tissue from all patients undergoing PKP surgery. Before surgery, we explained the purpose of the operation in detail. We obtained ethical approval from the local Medical Ethics Committee and received written informed consent from all patients who underwent PKP surgery and tissue biopsy.

Extracting bone tissue samples during PKP surgery is a well-established technique. According to the methods for extracting specimens in previous studies [10–12], all the biopsy specimens were obtained by using a Jamshidi needle (8-gauge Jamshidi needle, Medtronic, Minneapolis, USA) to access the fractured vertebral body (Fig. 1b). We extracted the tissue in the lumbar fractured area using the transpedicular approach. At the same time, to reduce the risk of thoracic puncture, we used the intercostal–transversal approach to obtain the tissue in the thoracic vertebral area. The two methods were used to extract the same amount of bone tissue in the vertebral fractured area, avoiding error in the quantitative analysis of the tissue biopsy. We used intraoperative fluoroscopy to ensure accurate tissue extraction and successful cement injection during the surgical procedure. All the biopsy specimens were fixed with formalin and embedded in paraffin [13]. After that, all paraffin sections were stained with haematoxylin and eosin after decalcified preparation [14, 15].

Quantitative analysis of bone tissue

We reviewed the medical records between June 2011 and September 2019 and collected all the paraffin sections of the included patients from the pathology department to perform histological analysis. We observed and recorded all the tissue images by using a microscope (BX51 optical microscope, Olympus, Tokyo, Japan) and microphotographic computer. Quantitative tissue analysis was performed by using Image-Pro Plus measurement software (version 6.0, Media Cybernetics, Rockville, USA). According to the definition criteria provided by the American Society for Bone and Mineral

Research nomenclature [16, 17], histomorphometric parameters were analysed and expressed: lamellar bone volume/tissue volume (LBV/TV, %), woven bone volume/tissue volume (WBV/TV, %), cancellous bone volume/tissue volume (BV/TV, %), necrotic bone volume/tissue volume (NBV/TV, %), fibrous tissue volume/tissue volume (FV/TV, %) and endochondral bone volume/tissue volume (EBV/TV, %).

Measurement of the percentage of BME

Before surgical treatment, all the patients received MRI examination to assess the degree of damage to the fractured vertebral bodies. Based on the standard protocol, we performed MRI examinations on a 1.5-T MR imaging scanner (Signa 1.5, GE Medical Systems, Milwaukee, USA). Standard T2-weighted spin-echo, fat-suppressed T2-weighted spin-echo and T1-weighted spin-echo sequences were performed in the sagittal orientation. According to the interpretation of BME provided by Voormolen [8], BME in the fractured vertebral body was defined as increased signal intensity on T2-weighted images and decreased signal intensity on T1-weighted images (Fig. 1c).

According to the measurement criteria reported by previous studies [18, 19], we observed fractured vertebrae from three different slices, including central slices and slices at the left and right pedicles. If the bone marrow oedema signal was diffuse, we calculated the percentage of BME in the central slice [18]. If the distribution of the bone marrow oedema pattern differed on these sagittal slices, we calculated the percentage of BME of the images with the broadest distribution [19]. The percentage of BME was assessed on sagittal images on T1-weighted images and T2-fat suppressed images (percentage of BME = area of increased signal on T2-weighted images or decreased signal on T1-weighted images/area of fractured vertebral body). The area of the bone marrow oedema signal and area of the vertebral body were measured by using Image-Pro Plus software (version 6.0, Media Cybernetics, Rockville, USA). Five radiologists assessed all the fractured vertebral bodies in a consensus reading to obtain the reference standard.

Assessment of the severity of back pain

The VAS has been widely used in clinical procedure to assess the degree of pain in patients [20]. In this study, we used the VAS approach to perform pain assessments when patients were diagnosed with OVCFs. To prevent the effect of analgesics on the accuracy of pain assessment, patients who received analgesic treatment within one day before the pain assessment were excluded from this study. After receiving an accurate pain assessment, we promptly performed analgesia treatment based on the severity of BP. The specific method of VAS assessment is shown in Fig. 1d.

Table 1 Comparisons of the histomorphometric parameters between the two groups in phases I and II

Phase I	BME ≤ 75% (N = 12)	BME > 75% (N = 45)	p
BV/TV (%)	14.11 ± 6.52	14.51 ± 6.12	0.992
FV/TV (%)	12.49 ± 7.37	25.68 ± 20.39	0.014
EBV/TV (%)	7.4 ± 8.32	4.09 ± 6.87	0.025
NBV/TV (%)	9.13 ± 6.41	8.18 ± 8.39	0.489
WBV/TV (%)	0.81 ± 2.8	0.69 ± 2.61	0.895
LBV/TV (%)	0	0	–
VAS score	7.93 ± 1.08	8.58 ± 1.54	0.039
Time (Days)	16.83 ± 6.16	9.04 ± 6.79	0.002
Phase II	BME ≤ 75% (N = 46)	BME > 75% (N = 16)	P
BV/TV (%)	13.61 ± 5.97	14.89 ± 6.54	0.479
FV/TV (%)	15.25 ± 13.28	23.92 ± 14.61	0.022
EBV/TV (%)	3.4 ± 5.39	4.38 ± 5.4	0.369
NBV/TV (%)	8.95 ± 10.16	8.85 ± 5.56	0.569
WBV/TV (%)	13.36 ± 10.38	15.08 ± 15.83	0.656
LBV/TV (%)	16.07 ± 10.96	10.41 ± 6.69	0.035
VAS score	6.94 ± 1.84	8.55 ± 0.83	0.001
Time (Days)	101.23 ± 55.78	50.63 ± 21.26	< 0.001

BV/TV: Cancellous bone volume/tissue volume, FV/TV: Fibrous tissue volume/tissue volume, EBV/TV: Endochondral bone volume/tissue volume, NBV/TV: Necrotic bone volume/tissue volume, WBV/TV: Woven bone volume/tissue volume, LBV/TV: Lamellar bone volume/tissue volume. All values are indicated as the mean ± standard deviation (SD)

According to previous studies reported on back pain [21, 22], VAS is represented by using a 10-cm horizontal line (0 = no pain to 10 = worst pain). The beginning of the line on the left side (0-cm point) represented no itching. The end of the line on the right side (10-cm point) represented the most severe itching. The middle part indicated different degrees of BP. As illustrated in Fig. 1d, part A (0 < VAS score ≤ 3) represents mild pain that can be tolerated. Part B (3 < VAS score ≤ 6) represents back pain that can be tolerated but seriously affects the quality of sleep, and part C (6 < VAS score ≤ 10) represents severe pain that cannot be tolerated. Before the pain assessment, we explained the operation method to all the patients in detail.

Statistical analysis

All variables were expressed as means ± standard deviations (SD). We used the Mann–Whitney U test to compare the differences between both groups. Spearman's correlation test was used to assess the correlations between VAS score and the percentage of BME in fractured vertebral bodies. $p < 0.05$ were considered statistically significant.

Results

Patients characteristics

A total of 208 elderly Chinese patients with OVCFs between June 2011 and September 2019 were retrospectively reviewed by medical records at our hospital. However, 89 patients were excluded from this study, and 119 elderly Chinese patients met the inclusion criteria and were included in the present study (Fig. 2). One hundred nineteen histologic samples were taken from the patients enrolled in the present study. Overall, 57 patients were included in phase I, and the mean fracture time was 10.68 ± 7.35 days. In this phase, 12 patients were grouped into the low-oedema group, and 45 patients were grouped into the high-oedema group. Furthermore, 62 patients were included in phase II, and the mean fracture period was 88.18 ± 53.9 days. During this phase, 46 patients were grouped into the low-oedema group, and 16 patients were grouped into the high-oedema group.

The VAS score was positively correlated with BME (Rs = 0.454, $p < 0.001$, $y = 2.7217 \cdot x + 60.272$, $R^2 = 0.1123$) in phase I. The percentage of BME was positively correlated with the VAS score (Rs = 0.609, $p < 0.001$,
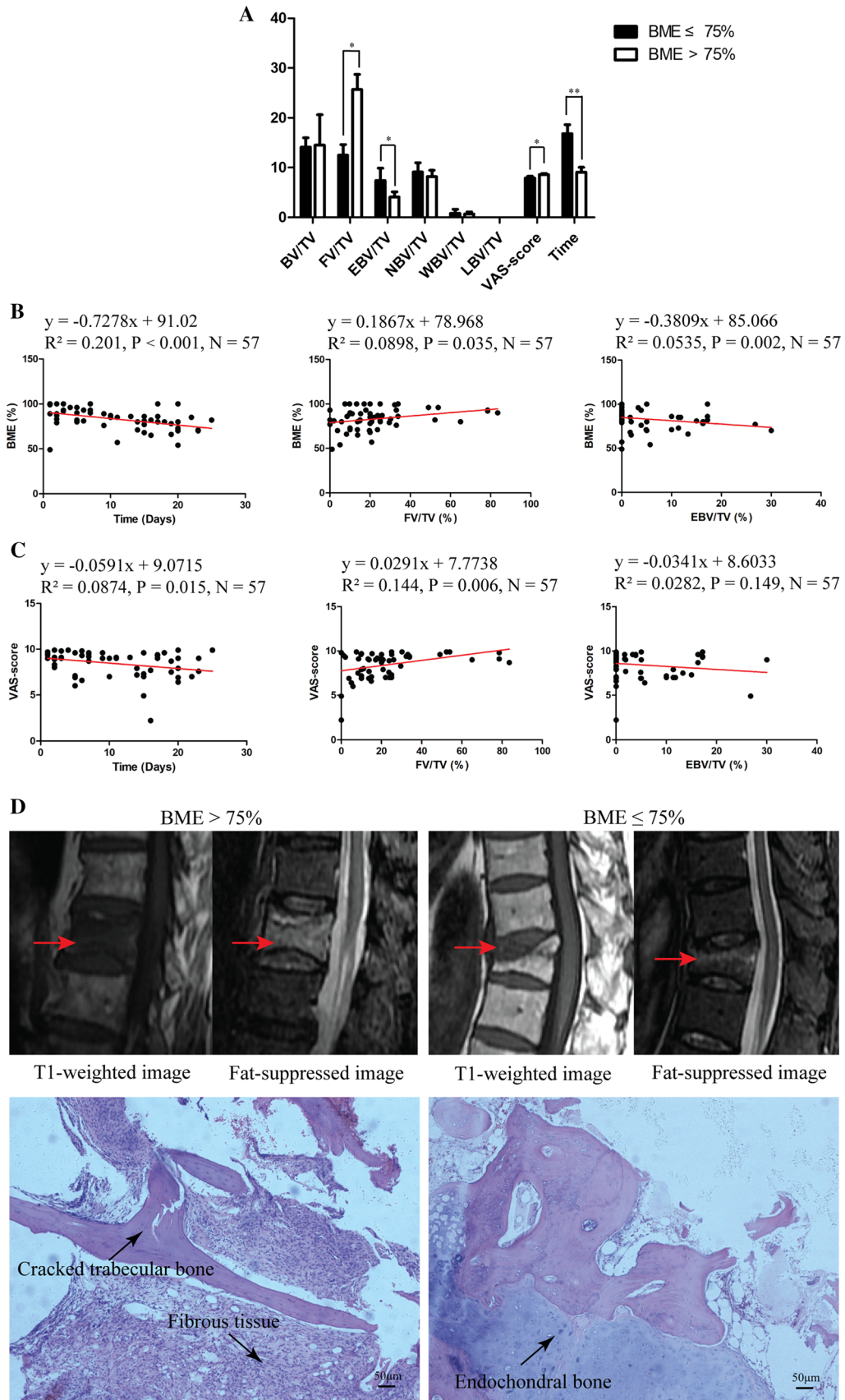
◄**Fig. 4** Differences between the groups in phase I. **a** Differences in the histomorphometric parameters between the groups in phase I; **b** Correlations between the percentage of BME and histomorphometric parameters in phase I; **c** Correlations between the VAS score and histomorphometric parameters in phase I; **d** Differences in tissue morphology and oedema signals on MRI between the groups in phase I. (A): BV/TV: Cancellous bone volume/tissue volume, FV/TV: Fibrous tissue volume/tissue volume, EBV/TV: Endochondral bone volume/tissue volume, NBV/TV: Necrotic bone volume/tissue volume, WBV/TV: Woven bone volume/tissue volume, LBV/TV: Lamellar bone volume/tissue volume. All values are indicated as the mean ± standard error of the mean (SEM). *$p < 0.05$, **$p < 0.01$, ***$p < 0.001$; (B): BME: bone marrow oedema

$y = 4.9468*x + 26.311$, $R^2 = 0.3375$) in phase II. The regression models are displayed in Fig. 3.

Patients in phase I

The differences in the clinical variables and histomorphometric parameters between the groups are summarized in Table 1 and Fig. 4a. The VAS score in the low-oedema group (7.93 ± 1.08) was significantly lower than that in the high-oedema group (8.58 ± 1.54, $p = 0.039$). A large amount of fibrous tissue was observed during phase I (Fig. 4d), and the content of fibrous tissue in the low-oedema group

Table 2 Correlations between the percentage of BME and histomorphometric parameters in phases I and II

Variables	Mean ± Standard deviation	Correlation coefficient	p
Phases I (N=57)			
NBV/TV (%)	8.39 ± 7.97	−0.170	0.207
BV/TV (%)	14.43 ± 6.15	−0.073	0.592
FV/TV (%)	22.9 ± 19.16	0.280	0.035
EBV/TV (%)	4.78 ± 7.25	−0.397	0.002
WBV/TV (%)	0.71 ± 2.63	0.023	0.864
LBV/TV (%)	0	–	–
VAS score	8.44 ± 1.47	0.454	<0.001
Time (days)	10.68 ± 7.35	−0.508	<0.001
Phases II (N=62)			
NBV/TV (%)	8.92 ± 9.15	0.018	0.890
BV/TV (%)	13.95 ± 6.09	0.055	0.671
FV/TV (%)	17.49 ± 14.05	0.262	0.040
EBV/TV (%)	3.65 ± 5.36	0.080	0.535
WBV/TV (%)	13.81 ± 11.9	0.001	0.994
LBV/TV (%)	14.61 ± 10.29	−0.379	0.002
VAS score	7.36 ± 1.78	0.609	<0.001
Time (days)	88.18 ± 53.89	−0.644	<0.001

BV/TV: Cancellous bone volume/tissue volume, FV/TV: Fibrous tissue volume/tissue volume, EBV/TV: Endochondral bone volume/tissue volume, NBV/TV: Necrotic bone volume/tissue volume, WBV/TV: Woven bone volume/tissue volume, LBV/TV: Lamellar bone volume/tissue volume

Table 3 Correlations between the VAS score and histomorphometric parameters in phases I and II

| Variables	Mean ± Standard deviation	Correlation coefficient	p
Phase I (N=57)			
NBV/TV (%)	8.39 ± 7.97	−0.047	0.729
BV/TV (%)	14.43 ± 6.15	−0.167	0.215
FV/TV (%)	22.9 ± 19.16	0.358	0.006
EBV/TV (%)	4.78 ± 7.25	−0.194	0.149
WBV/TV (%)	0.71 ± 2.63	0.082	0.543
LBV/TV (%)	0	–	–
Time (days)	10.68 ± 7.35	−0.321	0.015
Phase II (N=62)			
NBV/TV (%)	8.92 ± 9.15	0.046	0.725
BV/TV (%)	13.95 ± 6.09	0.158	0.221
FV/TV (%)	17.49 ± 14.05	0.269	0.035
EBV/TV (%)	3.65 ± 5.36	0.023	0.859
WBV/TV (%)	13.81 ± 11.9	−0.004	0.978
LBV/TV (%)	14.61 ± 10.29	−0.293	0.021
Time (days)	88.18 ± 53.89	−0.288	0.023

BV/TV: Cancellous bone volume/tissue volume, FV/TV: Fibrous tissue volume/tissue volume, EBV/TV: Endochondral bone volume/tissue volume, NBV/TV: Necrotic bone volume/tissue volume, WBV/TV: Woven bone volume/tissue volume, LBV/TV: Lamellar bone volume/tissue volume

($12.49 \pm 7.37\%$) was significantly lower than that in the high-oedema group ($25.68 \pm 20.39\%$, $p = 0.014$).

The correlations between the percentage of BME and histomorphometric parameters in phase I are summarized in Table 2. The percentage of BME was positively correlated with the content of fibrous tissue (Rs = 0.280, $p = 0.035$, $y = 0.1867*x + 78.968$, $R^2 = 0.0898$) and negatively correlated with endochondral bone (Rs = −0.397, $p = 0.002$, $y = -0.3809 *x + 85.066$, $R^2 = 0.0535$), and the regression models are displayed in Fig. 4b. The correlations between the degree of BP and histomorphometric parameters are summarized in Table 3. The VAS score was positively correlated with the content of fibrous tissue ($Rs = 0.358$, $p = 0.006$, $y = 0.0291*x + 7.7738$, $R^2 = 0.144$), and the regression models are displayed in Fig. 4c.

Patients in phase II

The differences in the histomorphometric parameters and clinical variables between the groups are summarized in Table 1 and Fig. 5a. The VAS score in the low-oedema group (6.94 ± 1.84) was significantly lower than that in the high-oedema group (8.55 ± 0.83, $p = 0.001$). Fibrous tissue could still be observed in phase II, and the content of fibrous tissue in the low-oedema group ($15.25 \pm 13.28\%$) was significantly lower than that in the high-oedema
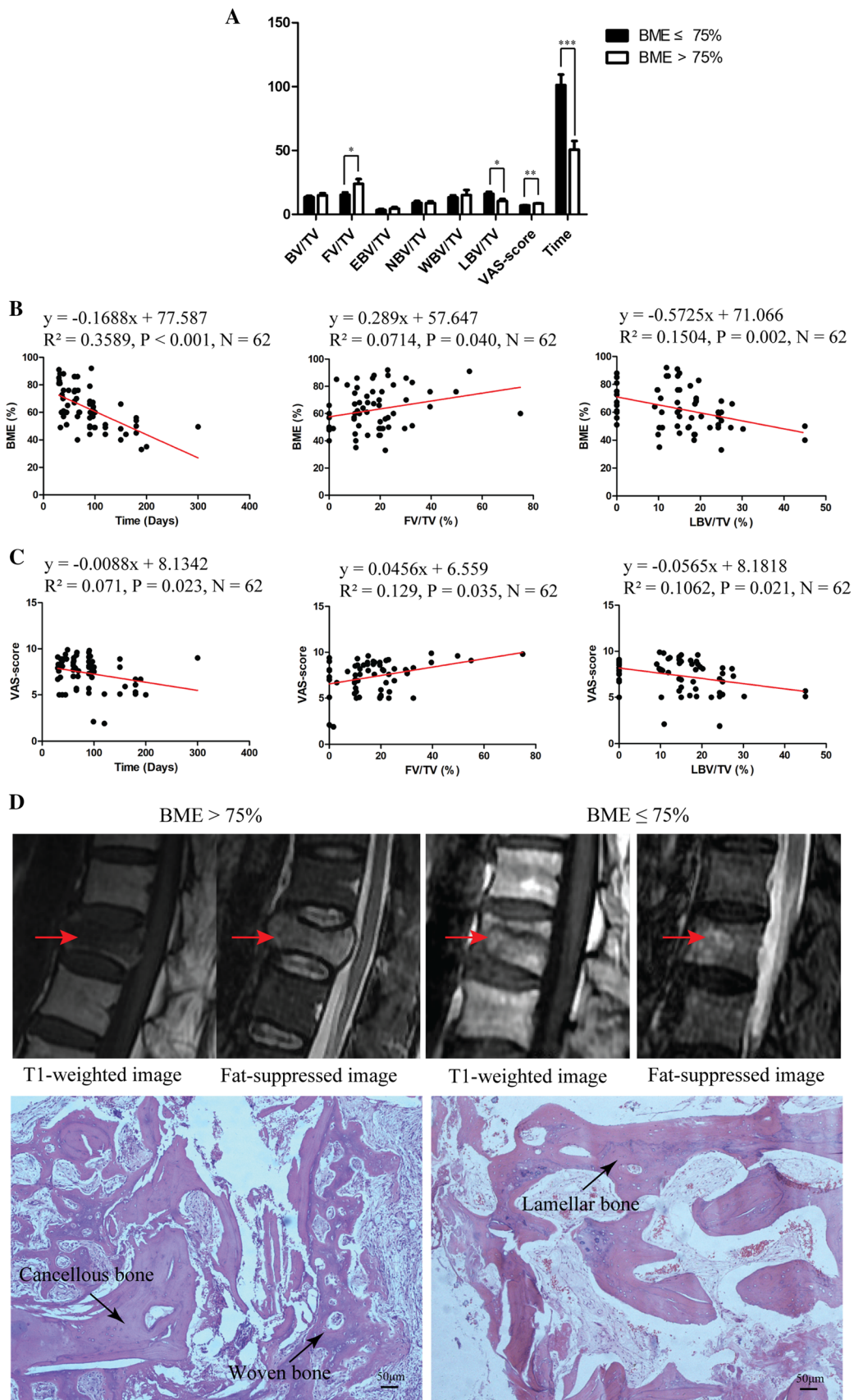
◀**Fig. 5** Differences in results between the groups in phase II. **a** Differences in the histomorphometric parameters between the groups in phase II; **b** Correlations between the percentage of BME and histomorphometric parameters in phase II; **c** Correlations between the VAS score and histomorphometric parameters in phase II; **d** Differences in tissue morphology and oedema signals on MRI between the groups in phase II. (A): BV/TV: Cancellous bone volume/tissue volume, FV/TV: Fibrous tissue volume/tissue volume, EBV/TV: Endochondral bone volume/tissue volume, NBV/TV: Necrotic bone volume/tissue volume, WBV/TV: Woven bone volume/tissue volume, LBV/TV: Lamellar bone volume/tissue volume. All values are indicated as the mean ± standard error of the mean (SEM). *$p<0.05$, **$p<0.01$, ***$p<0.001$; (B): BME: bone marrow oedema

group ($23.92 \pm 14.61\%$, $p = 0.022$). Additionally, immature woven bone and endochondral bone gradually mineralized to form lamellar bone in this phase (Fig. 5d). The content of lamellar bone in the low-oedema group ($16.07 \pm 10.96\%$) was significantly higher than that in the high-oedema group ($10.41 \pm 6.69\%$, $p = 0.035$).

In phase II, the correlations between the percentage of BME and histomorphometric parameters are summarized in Table 2. The percentage of BME was negatively correlated with the content of lamellar bone ($Rs = -0.379$, $p = 0.002$, $y = -0.5725 *x + 71.066$, $R^2 = 0.1504$) and positively correlated with fibrous tissue ($Rs = 0.262$, $p = 0.040$, $y = 0.289 *x + 57.647$, $R^2 = 0.0714$), and the regression models are displayed in Fig. 5b. The correlations between the histomorphometric parameters and degree of BP are summarized in Table 3. The VAS score was positively correlated with the fibrous tissue content ($Rs = 0.269$, $p = 0.035$, $y = 0.0456*x + 6.559$, $R^2 = 0.129$) and negatively correlated with the lamellar bone content ($Rs = -0.293$, $p = 0.021$, $y = -0.0565*x + 8.1818$, $R^2 = 0.1062$), and the regression models are displayed in Fig. 5c.

Discussion

MRI examinations combined with short tau inversion recovery (STIR) sequences and T1-weighted image sequences are very sensitive in assessing BME caused by fresh vertebral fractures [23]. However, the relationship between BME and BP is unclear. To clarify the specific mechanisms regarding these potential correlations between BP and BME, we used histomorphometric detection techniques to investigate the microarchitecture in fractured areas by quantitative analysis of bone tissue.

Relationships between the percentage of BME and time after fracture in patients with OVCFs

According to previous studies by Diamond et al. [10] and Haoran et al. [11], a stable OVCF healing process commonly comprises four stages. Consistent with histomorphological

kinetic features, the characteristics of BME signals on MRI gradually change at different stages of the healing process. Some researchers have deemed that the appearance of MRI during the fracture healing process can be divided into five stages based on the intensity of the BME signals [2]: 1. the occurrence of vertebral ischaemic changes; 2. the presentation of BME as high on T2-weighted imaging on MRI due to local bleeding and proliferation of fibrous tissue; 3. irregular enhancement at the fractured area caused by an increased blood supply; 4. BME signals gradually decrease as the blood supply recovers to normal levels; 5. some tissues in the fractured area are replaced by adipose tissue. Our results also support similar changes. In the current study, the percentage of BME was negatively correlated with the time after the original fracture in phases I ($Rs = -0.508$, $p < 0.001$, $y = -0.7278*x + 91.02$, $R^2 = 0.201$) and II ($Rs = -0.644$, $p < 0.001$, $y = -0.1688 *x + 77.587$, $R^2 = 0.3589$). These results suggest that the BME signal intensity gradually decreases during the healing process.

Relationships between the percentage of BME and degree of BP in patients with OVCFs

OVCFs, which may cause BP and limitations in mobility of the spine, are a severe clinical problem in the elderly population [24]. Sometimes, patients with OVCFs do not have definite localizing pain, and simple physical examination also makes it difficult to assess the specific fracture locations. Therefore, MRI is the most effective radiological examination to determine the location of the fractured vertebra and assess the degree of vertebral collapse [8]. Wei et al. deemed that a small range of oedema signals often leads to severe BP due to the unstable condition of spinal mechanics [2]. This unstable healing condition in the fractured area may aggravate the degree of BP. However, unlike the above views, we found a positive correlations between the percentage of BME and extent of BP in phases I ($Rs = 0.454$, $p < 0.001$, $y = 2.7217*x + 60.272$, $R^2 = 0.1123$) and II ($Rs = 0.609$, $p < 0.001$, $y = 4.9468*x + 26.311$, $R^2 = 0.3375$). To further explore the relevant mechanisms, we performed quantitative analysis of bone tissue at the fractured area. Quantitative analysis of the specimens showed that the content of fibrous tissue in the high-oedema group was significantly higher than that in the low-oedema group in phases I ($p = 0.014$) and II ($p = 0.022$). Additionally, the content of fibrous tissue was positively correlated with the percentage of BME ($Rs = 0.280$, $p = 0.035$, $y = 0.1867*x + 78.968$, $R^2 = 0.0898$) and the VAS score ($Rs = 0.358$, $p = 0.006$, $y = 0.0291*x + 7.7738$, $R^2 = 0.144$) in phase I. During phase II, the content of fibrous tissue was still positively correlated with the percentage of BME ($Rs = 0.262$, $p = 0.040$, $y = 0.289 *x + 57.647$, $R^2 = 0.0714$) and VAS score

(Rs = 0.269, $p = 0.035$, $y = 0.0456*x + 6.559$, $R^2 = 0.129$). These results suggested that a large amount of fibrous tissue in the fractured area likely caused the high intensity of BME signals during the fracture healing process. Thus, the large amount of tissue caused by the fresh fracture (hematoma and inflammatory factors) increased the water content of the fractured area, likely leading to an increase in the oedema signal in the fractured vertebra. Because of nociceptive nerve stimulation of the periosteum, the stimulation of inflammatory mediators may be the most important risk factor for the aggravation of BP.

Moreover, we found another interesting phenomenon in this study. Importantly, quantitative analysis of bone tissue showed that lamellar bone initially appeared in phase II. However, the content of lamellar bone in the high-oedema group ($10.41 \pm 6.69\%$) was significantly lower than that in the low-oedema group ($16.07 \pm 10.96\%$, $p = 0.035$) during the same period. To further analyse whether the content of lamellar bone affects oedema signals and BP, we assessed the correlations between the lamellar bone content and the percentage of BME and between the lamellar bone content and the VAS score separately. Spearman's correlation test showed that the lamellar bone content was negatively correlated with the percentage of BME (Rs = −0.379, $p = 0.002$, $y = −0.5725*x + 71.066$, $R^2 = 0.1504$) and VAS score (Rs = −0.293, $p = 0.021$, $y = −0.0565*x + 8.1818$, $R^2 = 0.1062$) in phase II. Based on the above results, we hypothesized that the supporting ability in the fractured area might be reduced because of less lamellar bone mineralized in the high-oedema group. This reduced supporting capacity of lamellar bone may increase the risk of microfractures. At the same time, fibrous tissue and inflammatory mediators may aggravate the degree of BP. Regarding the above hypothesis, many animal experiments may be required for further investigation.

In conclusion, this study is the first to analyse the mechanisms of these potential relationships between the percentage of BME and degree of BP using tissue biopsy. There are several innovations in our study. First, to investigate the correlations between BME and BP, we first used histomorphometric detection techniques, making the results more accurate and reliable. Second, we first found that the BME signals on MRI could be considered the most sensitive indicator to assess the degree of BP. Third, we investigated the relevant mechanisms regarding the potential correlations and proposed a new hypothesis for this interesting phenomenon. These findings are essential for the clinical diagnosis and treatment of complications such as BP and limitations in mobility with OVCFs. However, several limitations in our study should be mentioned. First, the percentage of BME in most patients was greater than 50%. For patients with a small range of BME, we usually recommend anti-osteoporosis therapy and conservative treatment based on the treatment guidelines for osteoporotic fractures [25, 26], making it impossible to extract bone tissue specimens from the fractured vertebra. Second, we only measured the content of bone tissue in the fractured area and did not include other clinical variables that may reflect the fracture healing process, such as bone turnover markers and bone mineral density. To further investigate the healing process of OVCFs, we will further analyse the impact of other clinical variables, such as bone turnover markers and bone mineral density, on the assessment of BP in future studies. Finally, to reduce the influence of fractured segments on tissue morphology, we analysed only patients with thoracolumbar fractures. In future studies, we will analyse the impact of fracture segments on tissue morphology and imaging features during the healing process.

Conclusions

Oedema signals on MRI can be considered a sensitive indicator to assess the degree of BP, and fibrous tissue may be one of the most important risk factors for the aggravation of BP and BME. Additionally, we proposed a new hypothesis for this interesting phenomenon: delayed mineralization may increase the degree of BP due to microfractures.

Declarations

Conflict of interest There is no conflict of interest among the authors.

Ethical approval Permission to conduct this retrospective study was obtained from the authors' hospital ethics committee.

Consent to participate All the patients included consent to participate in the retrospective study.

Consent for publication All the patients included, as well as the hospital ethics committee, con consent for publication of the retrospective study.

References

1. Hall SE, Criddle RA, Comito TL, Prince RL (1999) A case-control study of quality of life and functional impairment in women with long-standing vertebral osteoporotic fracture. Osteoporos int 9:508–515. https://doi.org/10.1007/s001980050178

2. Xu W, Wang S, Chen C, Li Y, Ji Y, Zhu X, Li Z (2018) Correlation analysis between the magnetic resonance imaging characteristics of osteoporotic vertebral compression fractures and the efficacy of percutaneous vertebroplasty: a prospective cohort study. BMC Musculoskelet Disord 19:114. https://doi.org/10.1186/s12891-018-2040-8

3. Mattie R, Laimi K, Yu S, Saltychev M (2016) Comparing percutaneous vertebroplasty and conservative therapy for treating osteoporotic compression fractures in the thoracic and lumbar spine: a systematic review and meta-analysis. J Bone Joint Surg Am 98:1041–1051. https://doi.org/10.2106/JBJS.15.00425

4. Kim JH, Kim JI, Jang BH, Seo JG, Kim JH (2010) The comparison of bone scan and MRI in osteoporotic compression fractures. Asian Spine J 4:89–95. https://doi.org/10.4184/asj.2010.4.2.89

5. Alvarez L, Pérez-Higueras A, Granizo JJ, de Miguel I, Quiñones D, Rossi RE (2005) Predictors of outcomes of percutaneous vertebroplasty for osteoporotic vertebral fractures. Spine (Phila Pa 1976) 30:87–92. https://doi.org/10.1097/00007632-200501010-00016

6. Brown DB, Glaiberman CB, Gilula LA, Shimony JS (2005) Correlation between preprocedural MRI findings and clinical outcomes in the treatment of chronic symptomatic vertebral compression fractures with percutaneous vertebroplasty. AJR Am J Roentgenol 184:1951–1955. https://doi.org/10.2214/ajr.184.6.01841951

7. Glaser DL, Kaplan FS (1997) Osteoporosis. Definition and clinical presentation. Spine (Phila Pa 1976) 22:12S-16S. https://doi.org/10.1097/00007632-199712151-00003

8. Voormolen MH, van Rooij WJ, van der Graaf Y, Lohle PN, Lampmann LE, Juttmann JR, Sluzewski M (2006) Bone marrow edema in osteoporotic vertebral compression fractures after percutaneous vertebroplasty and relation with clinical outcome. AJNR Am J Neuroradiol 27:983–988

9. Zhang L, Li J, Yang H, Luo Z, Zou J (2013) Histological evaluation of bone biopsy results during PVP or PKP of vertebral compression fractures. Oncol lett 5:135–138. https://doi.org/10.3892/ol.2012.944

10. Diamond TH, Clark WA, Kumar SV (2007) Histomorphometric analysis of fracture healing cascade in acute osteoporotic vertebral body fractures. Bone 40:775–780. https://doi.org/10.1016/j.bone.2006.10.009

11. Qi H, Xue J, Gao J, Zhang Y, Sun J, Wang G (2020) Changes of bone turnover markers and bone tissue content after severe osteoporotic vertebral compression fracture. Med Sci Monit 26:e923713. https://doi.org/10.12659/MSM.923713

12. Diamond TH, Champion B, Clark WA (2003) Management of acute osteoporotic vertebral fractures: a nonrandomized trial comparing percutaneous vertebroplasty with conservative therapy. Am J Med 114:257–265. https://doi.org/10.1016/s0002-9343(02)01524-3

13. Sadeghipour A, Babaheidarian P (2019) Making formalin-fixed, paraffin embedded blocks. Methods Mol Biol 1897:253–268. https://doi.org/10.1007/978-1-4939-8935-5_22

14. Diamond TH, Stiel D, Lunzer M, McDowall D, Eckstein RP, Posen S (1989) Hepatic osteodystrophy. Static and dynamic bone histomorphometry and serum bone Gla-protein in 80 patients with chronic liver disease. Gastroenterology 96:213–221

15. Sy J, Ang LC (2019) Microtomy: cutting formalin-fixed, paraffin-embedded sections. Methods Mol Biol 1897:269–278. https://doi.org/10.1007/978-1-4939-8935-5_23

16. Einhorn TA (1998) The cell and molecular biology of fracture healing. Clin Orthop Relat Res 1998:S7-21. https://doi.org/10.1097/00003086-199810001-00003

17. Einhorn TA (2005) The science of fracture healing. J Orthop Trauma 19:S4-6. https://doi.org/10.1097/00005131-200511101-00002

18. Zhang Y, Qi H, Zhang Y, Wang J, Xue J (2021) Vertebral bone marrow edema in magnetic resonance imaging correlates with bone healing histomorphometry in (sub)acute osteoporotic vertebral compression fracture. Eur Spine J 30:2708–2717. https://doi.org/10.1007/s00586-021-06814-3

19. Tanigawa N, Komemushi A, Kariya S, Kojima H, Shomura Y, Ikeda K, Omura N, Murakami T (2006) Percutaneous vertebroplasty: relationship between vertebral body bone marrow edema pattern on MR images and initial clinical response. Radiology 239:195–200. https://doi.org/10.1148/radiol.2391050073

20. Bergasa NV, Talbot TL, Alling DW, Schmitt JM, Walker EC, Baker BL, Korenman JC, Park Y (1992) A controlled trial of naloxone infusions for the pruritus of chronic cholestasis. Gastroenterology 102:544–549. https://doi.org/10.1016/0016-5085(92)90102-5

21. Chen F, Xin J, Su C, Liu X, Cui X (2021) Pain variability of tissues under endoscope in percutaneous endoscopic lumbar discectomy and its significance: a retrospective study. Pain Physician 24:E877–E882

22. Xin J, Liu X, Jing X, Su C, Mao Y, Chen F, Wang W, Cui X (2021) Multifactor analysis of costal pain in osteoporotic fracture of thoracic vertebra. Pain Physician 24:E795–E802

23. Spiegl UJ, Beisse R, Hauck S, Grillhösl A, Bühren V (2009) Value of MRI imaging prior to a kyphoplasty for osteoporotic insufficiency fractures. Eur Spine J 18:1287–1292. https://doi.org/10.1007/s00586-009-1045-2

24. Yuan WH, Teng MM, Hsu HC, Sun YC, Chang CY (2008) Are non-contrast MR images enough for detection of fracture levels prior to percutaneous vertebroplasty in patients with osteoporosis? Interv Neuroradiol 2008:79–84. https://doi.org/10.1177/15910199080140S214

25. Esses SI, McGuire R, Jenkins J, Finkelstein J, Woodard E, Watters WC, Goldberg MJ, Keith M (2011) The treatment of symptomatic osteoporotic spinal compression fractures. J Am Acad Orthop Surg 19:176–182. https://doi.org/10.5435/00124635-201103000-00007

26. Leali PT, Solla F, Maestretti G, Balsano M, Doria C (2016) Safety and efficacy of vertebroplasty in the treatment of osteoporotic vertebral compression fractures: a prospective multicenter international randomized controlled study. Clin Cases Miner Bone Metab 13:234–236. https://doi.org/10.11138/ccmbm/2016.13.3.234